Обзор ArXiv: astro-ph, 4-8мая 2020

От Сильченко О.К.

ArXiv: 2005.01724

Massive disc galaxies in cosmological hydrodynamical simulations are too dark matter-dominated

A. Marasco[1], L. Posti[2], K. Oman[3], B. Famaey[2], G. Cresci[1] and F. Fraternali[4]

[1] INAF - Osservatorio Astrofisico di Arcetri, Largo E. Fermi 5, 50127, Firenze, Italy
e-mail: antonino.marasco@inaf.it
[2] Université de Strasbourg, CNRS UMR 7550, Observatoire astronomique de Strasbourg, 11 rue de l'Université, 67000 Strasbourg, France
[3] Institute for Computational Cosmology, Department of Physics, Durham University, South Road, Durham DH1 3LE, UK
[4] Kapteyn Astronomical Institute, University of Groningen, Postbus 800, 9700 AV Groningen, The Netherlands

Received ; accepted

ABSTRACT

We investigate the disc-halo connection in massive ($M_\star > 5 \times 10^{10}\,M_\odot$) disc galaxies from the cosmological hydrodynamical simulations EAGLE and IllustrisTNG, and compare it with that inferred from the study of H I rotation curves in nearby massive spirals from the Spitzer Photometry and Accurate Rotation Curves (SPARC) dataset. We find that discrepancies between the the simulated and observed discs arise both on global and on local scales. Globally, the simulated discs inhabit halos that are a factor ~ 4 (in EAGLE) and ~ 2 (in IllustrisTNG) more massive than those derived from the rotation curve analysis of the observed dataset. We also use synthetic rotation curves of the simulated discs to demonstrate that the recovery of the halo masses from rotation curves are not systematically biased. We find that the simulations predict dark-matter dominated systems with stellar-to-total enclosed mass ratios that are a factor of 1.5 – 2 smaller than real galaxies at all radii. This is an alternative manifestation of the 'failed feedback problem', since it indicates that simulated halos hosting massive discs have been too inefficient at converting their baryons into stars, possibly due to an overly efficient stellar and/or AGN feedback implementation.

Выборка SPARC

Galaxy (1)	$\log_{10}(M_\star/M_\odot)$ (2)	$\epsilon_{M_\star,\mathrm{low}}$ (3)	$\epsilon_{M_\star,\mathrm{up}}$ (4)	$\log_{10}(M_{\mathrm{halo}}/M_\odot)$ (5)	$\epsilon_{M_{\mathrm{halo}},\mathrm{low}}$ (6)	$\epsilon_{M_{\mathrm{halo}},\mathrm{up}}$ (7)	v_{flat} (8)	$\epsilon_{v_{\mathrm{flat}}}$ (9)	R_{eff} (10)	$\epsilon_{R_{\mathrm{eff}}}$ (11)
NGC 7331	10.78	10.69	10.84	12.38	12.21	12.60	239.00	5.40	3.99	0.41
NGC 5985	10.91	10.55	11.10	12.21	12.12	12.28	293.60	8.60	10.71	2.67
UGC 03205	10.94	10.85	11.00	12.12	11.95	12.33	219.60	8.60	5.35	1.07
UGC 11914	10.95	10.82	11.04	13.04	12.44	13.67	288.10	10.50	3.12	0.94
UGC 05253	10.95	10.81	11.05	12.16	12.08	12.27	213.70	7.10	4.28	1.07
NGC 5907	10.96	10.87	11.01	12.02	11.93	12.16	215.00	2.90	7.88	0.41
NGC 2998	10.98	10.85	11.07	12.01	11.91	12.13	209.90	8.10	7.06	1.06
NGC 2841	11.00	10.95	11.04	12.54	12.42	12.69	284.80	8.60	5.51	0.55
NGC 3992	11.01	10.93	11.07	12.15	12.03	12.30	241.00	5.20	9.99	0.97
UGC 12506	11.12	10.95	11.19	12.14	11.96	12.33	234.00	16.80	12.36	1.24
NGC 5371	11.13	10.94	11.26	11.64	11.53	11.74	209.50	3.90	9.80	2.45
UGC 09133	11.15	11.04	11.24	12.22	12.18	12.25	226.80	4.20	5.92	1.18
NGC 2955	11.17	11.11	11.22	12.13	11.80	12.48	– [a]	– [a]	7.22	0.72
UGC 02953	11.18	11.03	11.28	12.29	12.22	12.36	264.90	6.00	5.03	1.51
NGC 6195	11.21	11.15	11.26	12.16	11.94	12.42	251.70	9.30	9.52	0.95
UGC 11455	11.22	11.11	11.31	12.61	12.43	12.84	269.40	7.40	10.06	1.51
NGC 0801	11.23	11.18	11.28	12.00	11.90	12.14	220.10	6.20	7.76	0.78
NGC 6674	11.24	11.15	11.32	12.42	12.32	12.56	241.30	4.90	7.75	1.54
UGC 02885	11.37	11.30	11.43	12.62	12.48	12.79	289.50	12.00	12.20	1.22
UGC 02487	11.39	11.33	11.45	12.58	12.52	12.67	332.00	3.50	9.63	1.45
ESO 563-G021	11.40	11.33	11.46	12.93	12.70	13.21	314.60	11.70	10.59	1.59

Notes. (1) Galaxy name; (2)-(4) stellar mass and related lower and upper uncertainties from PFM19; (5)-(7) halo mass and related lower and upper uncertainties from PFM19; (8)-(9) velocity of the flat part of the rotation curve (in $\mathrm{km\,s^{-1}}$) and related uncertainty from Lelli et al. (2016); (6) effective radius (in kpc) and related uncertainty from Lelli et al. (2016).

[a] The rotation curve of NGC 2955 does not have a well defined flat part, thus its v_{flat} is not reported in Lelli et al. (2016).

Аналогичная выборка модельных галактик

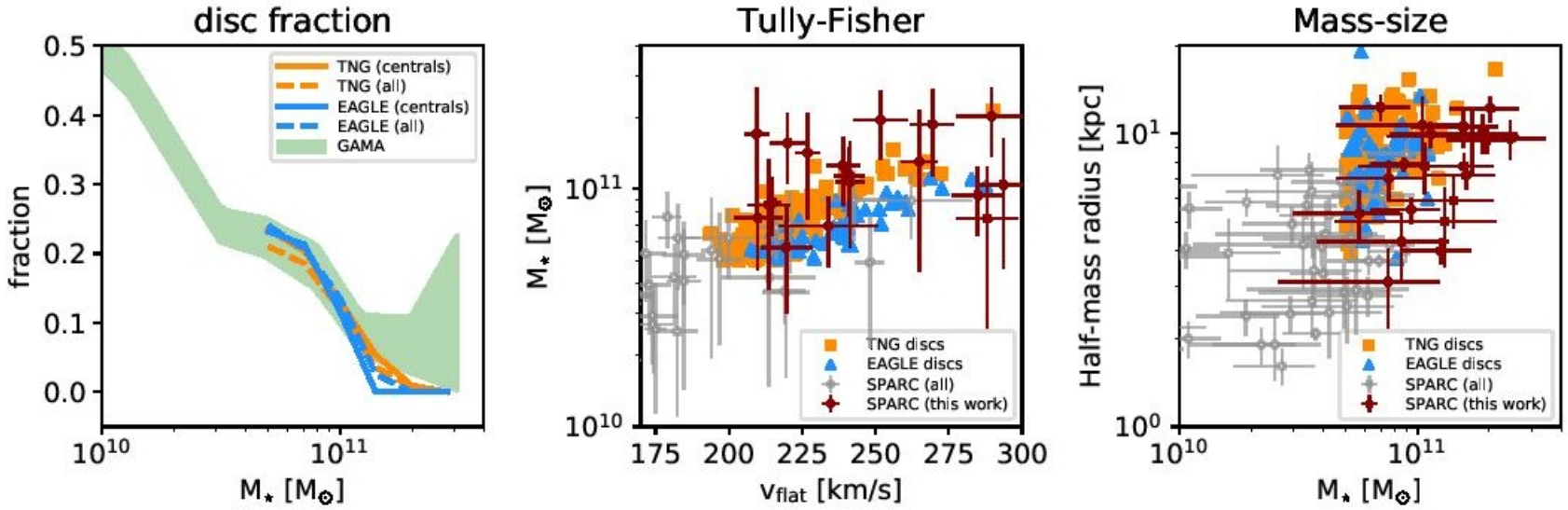

Fig. 1. *Left panel:* fraction of disc galaxies as a function of their stellar mass in EAGLE (blue lines) and IllustrisTNG (orange lines), compared to that measured in the GAMA survey by Moffett et al. (2016, shaded green area). Solid lines show centrals only; dashed lines include also satellites. *Central panel:* stellar Tully-Fisher relation for our subsample of simulated (central) discs with $M_\star > 5 \times 10^{10}\,M_\odot$ in EAGLE (blue triangles) and IllustrisTNG (orange squares), compared with the population of nearby spirals from the SPARC dataset (circles with error bars). Galaxies from SPARC are shown as circles with error-bars. Filled red circles are used for the sub-sample of massive discs studied in this work. *Right panel:* stellar mass-size relation for the same systems.

В реальных галактиках больше барионов, чем в модельных

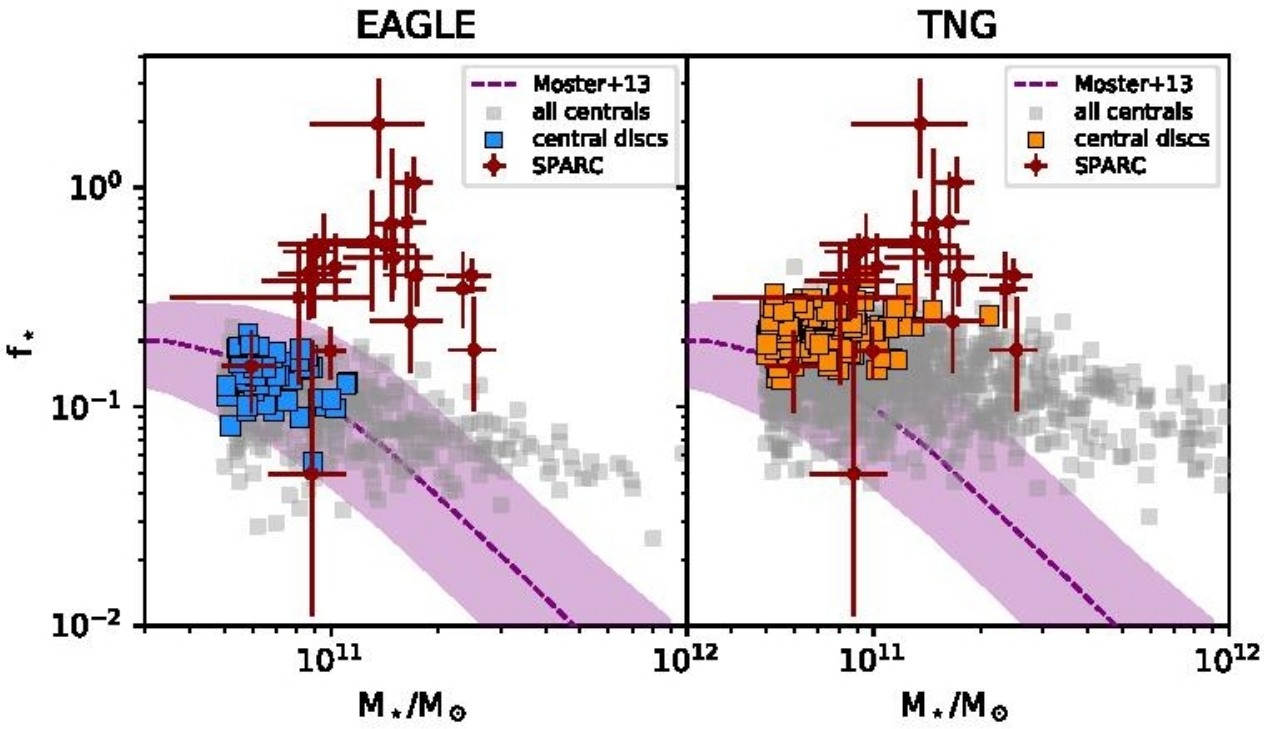

Fig. 2. Stellar fraction as a function of the stellar mass for simulated (central) galaxies in EAGLE (left panel) and IllustrisTNG (right panel) with $M_\star > 5 \times 10^{10}\,M_\odot$, compared to nearby spirals from the SPARC dataset (red circles with error-bar). Coloured symbols are used for our subsample of simulated discs. The purple shaded region shows the AM relation and related scatter from Moster et al. (2013).

… на всех расстояниях от центра!

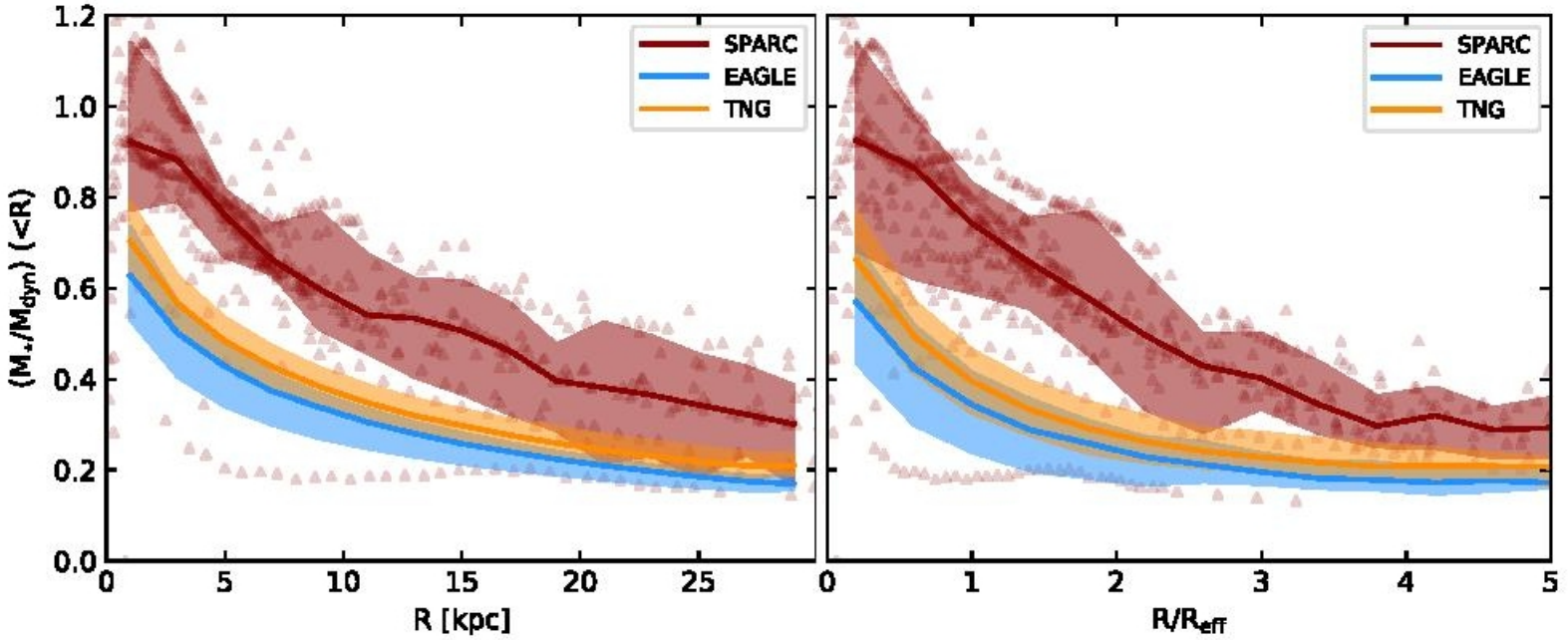

Fig. 3. *Left panel*: Stellar-to-total enclosed mass profiles for massive disc galaxies in the EAGLE (blue) and IllustrisTNG (orange) simulations, compared with the data from SPARC (red). The solid lines show the median profiles, while the shaded areas represent the scatter given by the difference between the 84th and the 16th percentiles. Individual measurements for SPARC spirals are shown as red triangles. *Right panel*: As in the left panel, but radii are normalised to the effective radius $R_{\rm eff}$ of each galaxy.

ArXiv: 2005.02355

Atomic Hydrogen Clues to the Formation of Counterrotating Stellar Discs

Lisa M. Young,[1,2]★ Davor Krajnović,[3] Pierre-Alain Duc,[4] and Paolo Serra[5]
[1] *Physics Department, New Mexico Tech, 801 Leroy Place, Socorro, NM 87801 USA*
[2] *Adjunct Astronomer, National Radio Astronomy Observatory*
[3] *Leibniz-Institut für Astrophysik Potsdam (AIP), An der Sternwarte 16, D-14482 Potsdam, Germany*
[4] *Observatoire Astronomique de Strasbourg, Université de Strasbourg, CNRS, UMR 7550, 11 rue de l'Université, F-67000 Strasbourg, France*
[5] *INAF - Osservatorio Astronomico di Cagliari, Via della Scienza 5, I-09047 Selargius (CA), Italy*

Accepted 2020 May 4. Received 2020 April 17; in original form 2020 February 14

ABSTRACT

We present interferometric HI observations of six double-disc stellar counterrotator ("2σ") galaxies from the ATLAS^{3D} sample. Three are detected in HI emission; two of these are new detections. NGC 7710 shows a modestly asymmetric HI disc, and the atomic gas in PGC 056772 is centrally peaked but too poorly resolved to identify the direction of rotation. IC 0719, the most instructive system in this study, shows an extended, strongly warped disc of ~ 43 kpc diameter, with a faint tail extending towards its neighbor IC 0718. The gas has likely been accreted from this external source during an encounter whose geometry directed the gas into misaligned retrograde orbits (with respect to the primary stellar body of IC 0719). In the interior, where dynamical time-scales are shorter, the HI has settled into the equatorial plane forming the retrograde secondary stellar disc. This is the first direct evidence that a double-disc stellar counterrotator could be formed through the accretion of retrograde gas. However, the dominant formation pathway for the formation of 2σ galaxies is still

Полная выборка контрвращающихся дисков в S0.

Table 1. Cold gas data for 2σ galaxies.

Name	log $M_\star$ ($M_\odot$)	log M(H_2) ($M_\odot$)	log M(HI) ($M_\odot$)	HI refs	Formation	Formation references
IC 0719	10.31	8.26 (0.04)	9.03 (0.02)	*	gas accretion	Katkov et al. (2013), Pizzella et al. (2018)
NGC 0448	10.43	< 7.74	< 7.38	*	merger	Katkov et al. (2016), Nedelchev et al. (2019)
NGC 3796	9.97	< 7.51	< 7.10	S12		
NGC 4191	10.47	< 7.94	9.57 (0.01)	Y18	gas accretion	Coccato et al. (2015), Young et al. (2018)
NGC 4259	10.10	< 7.97	< 8.43	*		
NGC 4473	10.73	< 7.07	< 6.86	S12		
NGC 4528	10.05	< 7.15	< 7.18	S12		
NGC 4550	10.13	6.91 (0.08)	< 6.89	S12	merger	Crocker et al. (2009), Coccato et al. (2013), Johnston et al. (2013)
NGC 4803	10.14	< 7.98	< 7.57	*		
NGC 7710	10.02	< 7.80	8.74 (0.02)	*	gas accretion?	*
PGC 056772	10.05	8.19 (0.05)	8.11 (0.06)	*	gas accretion?	*

Stellar masses are from (Cappellari et al. 2013). H_2 masses are all from Young et al. (2011), except NGC 4550 from Crocker et al. (2009).

HI references: * = This paper; S12 = Serra et al. (2012); Y18 = Young et al. (2018).

Наблюдения на VLT в 12см

3 OBSERVATIONS

IC 0719, NGC 0448, NGC 4803, NGC 7710, and PGC 056772 were observed with the Karl G. Jansky Very Large Array (VLA) in September 2018, in project 18A-226, for a total of two hours each (and four hours on NGC 7710). These data were obtained in the D configuration, giving baselines from 0.2 to 5 kλ and resolutions on the order of an arcminute. The native velocity resolution of the data is 3.3 km s^{-1}. The flux, bandpass, and time-dependent gain

Нашли HI в трех из шести!

NGC 7710

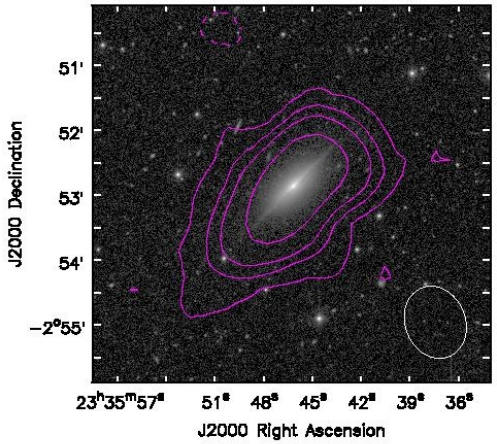

Figure 1. HI integrated intensity in NGC 7710. The grayscale is the MATLAS g image from Duc et al. (2015), and the contours are the HI column density at levels of $(-1, 1, 3, 5, 10, 30) \times 1.41 \times 10^{19}$ cm^{-2}, where $1.41{\times}10^{19}$ cm^{-2} is the nominal sensitivity in these data (Table 2). The resolution of the HI data is indicated by the ellipse in the lower right corner.

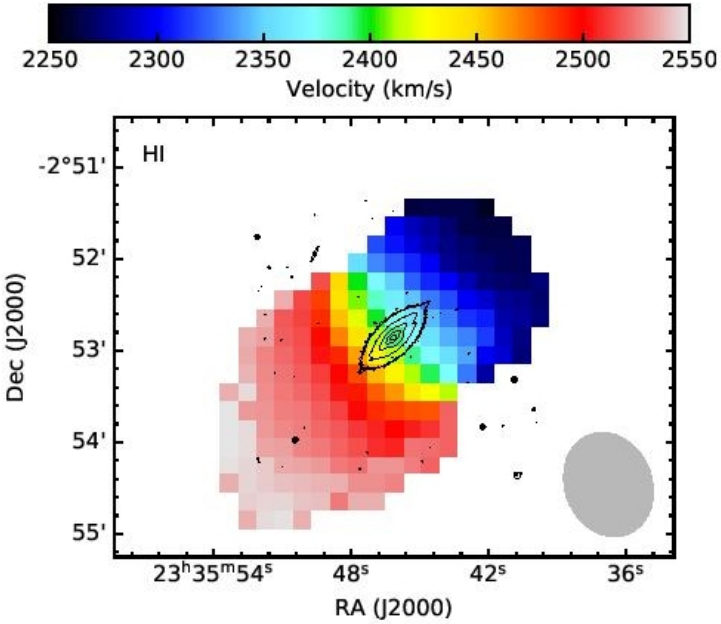

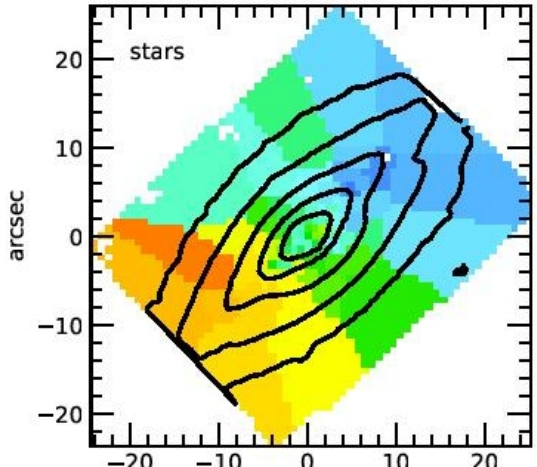

PGC 56772

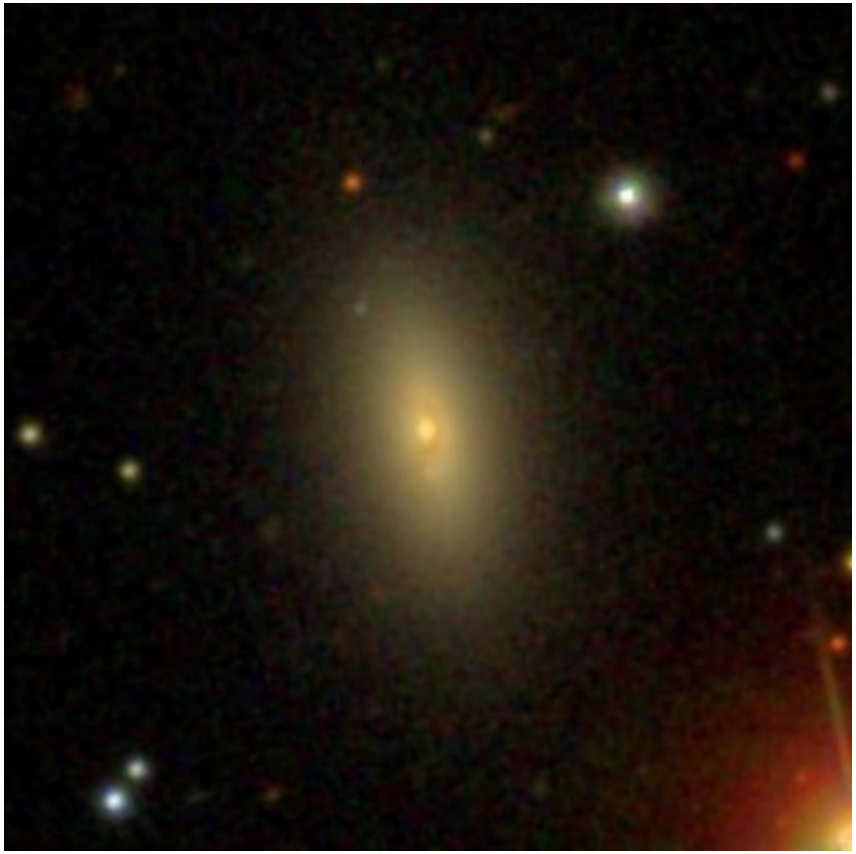

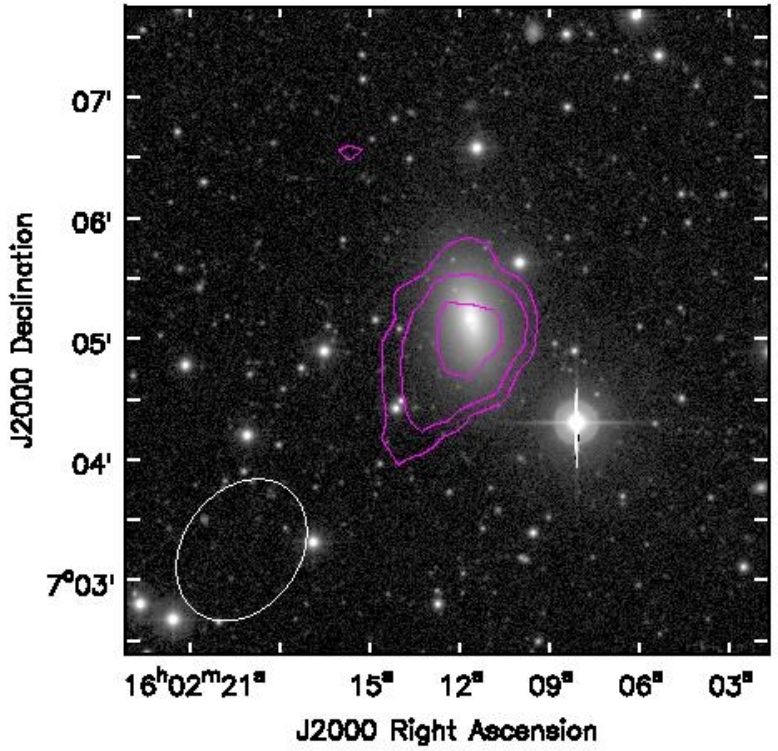

Figure 4. HI integrated intensity in PGC 056772. The grayscale is the MATLAS g image (Duc et al. 2015), and the contours are the HI column density at levels of $(1, 2, 4)\times 1.36\times 10^{19}$ cm^{-2}, which is the nominal sensitivity in these data. The resolution of the HI data is indicated by the ellipse in the lower left corner.

IC 719

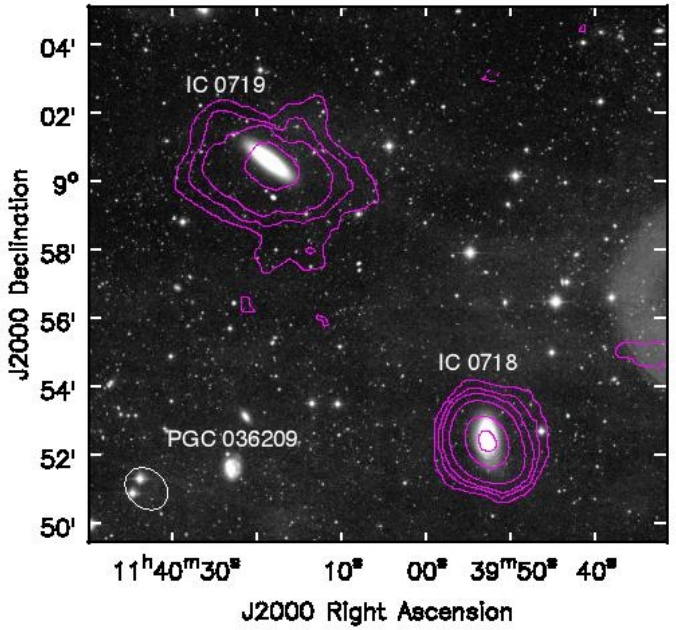

Figure 8. HI in IC 0719 and IC 0718. The optical image is the MATLAS r image (Duc et al. 2015). Contours are $(-1, 1, 3, 5, 10, 30, 50) \times 1.2 \times 10^{19}$ cm^{-2}, where 1.2×10^{19} cm^{-2} is the nominal sensitivity in this image (Table 2). PGC 036209 has a much higher velocity of 6372 km s^{-1} (Haynes et al. 2018) so it is a distant background object.

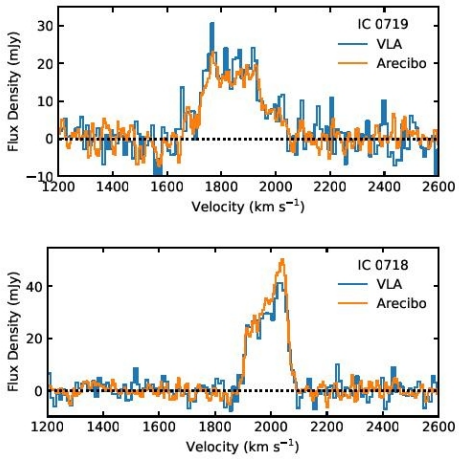

Figure 7. Integrated HI spectra of IC0719 and IC0718 from the VLA data and from Arecibo (Haynes et al. 2018).

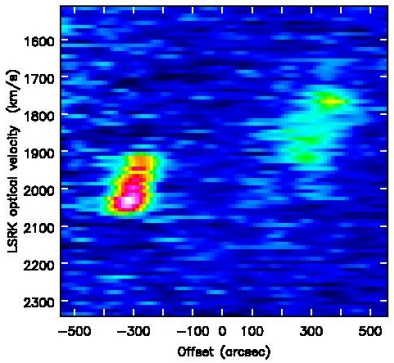

Figure 9. Position-velocity slice between IC 0718 (left) and IC 0719 (right). In this slice the emission is averaged over a region 204″ wide (~ 2.5 beams).

IC 718

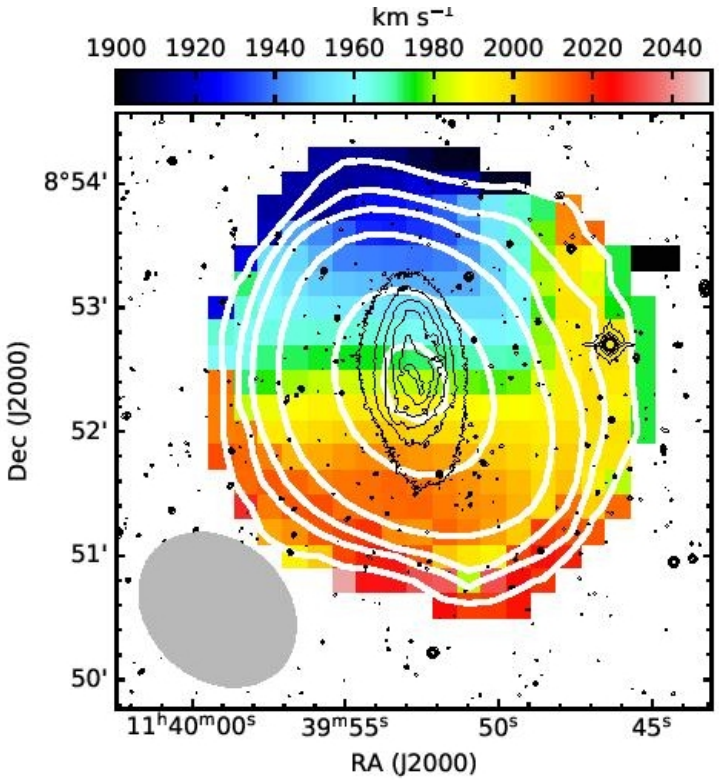

Figure 12. Velocity field of IC 0718 (neighbor to IC 0719). Thick white contours are the HI column density, as in Figure 8, and thin black contours are from the MATLAS *g* image. The beam size is indicated by the gray ellipse.

А вот то же самое - Arecibo

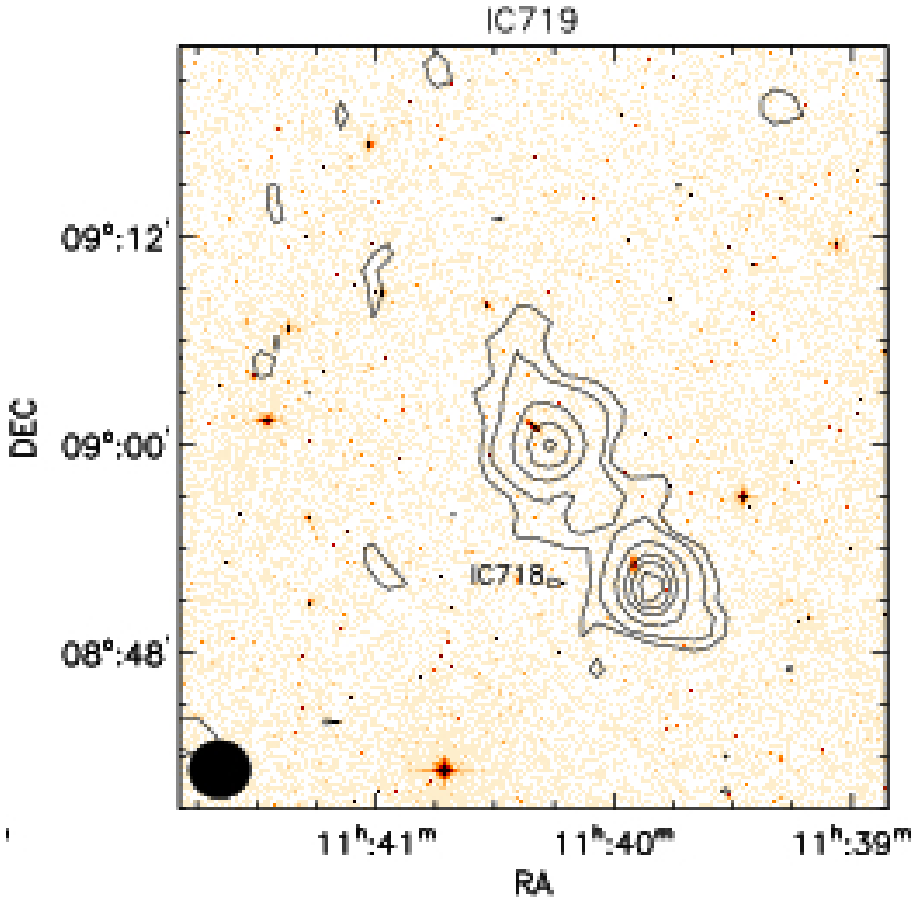

Откуда аккреция? С IC 718? Другая ориетация диска HI. Из филамента? Но тогда она полярная!!

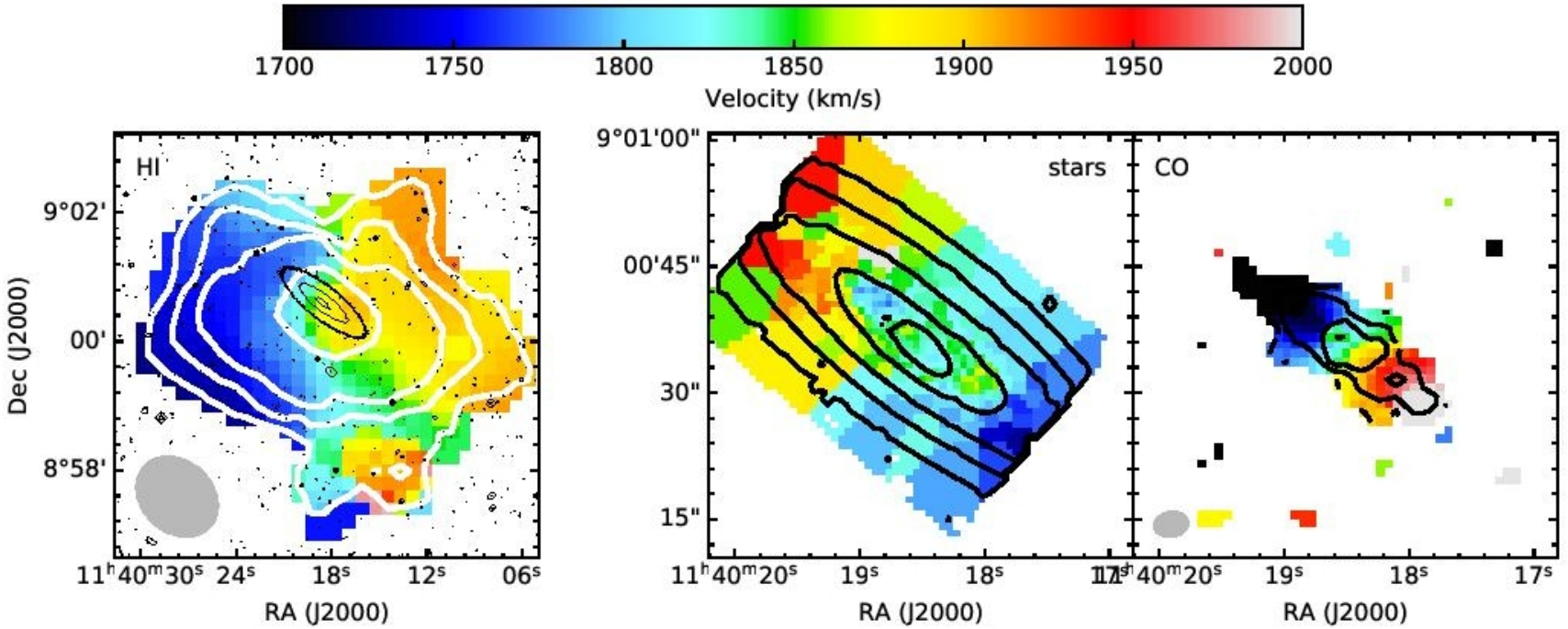

Figure 10. HI, stellar and CO velocity fields of IC 0719. For HI, the white contours show the column density as in Figure 8 and the black contours are from the optical image to show where the main stellar body of the galaxy is located. In the stellar velocities (centre panel), the black contours are again the stellar surface brightness. The primary stellar component defined by Pizzella et al. (2018) is receding on the northeast side of the galaxy; the secondary component is receding on the southwest side of the galaxy. The secondary component dominates the stellar velocity measurements in the annulus between the highest contour and the second-highest contour (radii 4″ to 10″); the primary component dominates both at smaller radii and at larger radii. In the CO field, black contours show the integrated CO surface brightness. Beam sizes are indicated by the ellipses.